Calculation and Analysis of Shielding Effectiveness of the Rectangular Enclosure with Apertures

Chuan-Chuan Wang[1], Chang-Qing Zhu[1], Xing Zhou[2], and Zhi-Feng Gu[1]

[1] Department of Electrical Engineering
Shi Jia Zhuang Mechanical Engineering College, Shi Jia Zhuang, 050003, P.R.China
wangchuan1083@126.com, zhuneil@163.com, gzfgohappy@163.com

[2] Electrostatic and Electromagnetic Research Institute
Shi Jia Zhuang Mechanical Engineering College, Shi Jia Zhuang, 050003, P.R.China
zxlwbh@126.com

Abstract ─ Based on transmission line theory, an approach which combines the analytical model developed by Robinson *et al*. and the model which analyses the shielding effectiveness (SE) of enclosure with an off-centre aperture or aperture array is presented. The model is more general than other methods and includes the incident wave with varied polarization angles and incident angles. It is quicker to calculate the SE with this model, which on the other hand enables to investigate the effect of important design parameters on SE. This model is validated by comparing the SE predictions with those from literatures. Different aspects' effect on the SE are investigated such as aperture dimension, enclosure dimension, position of observation point, number of apertures, polarization angles, and incident angles, etc.

Index Terms ─ Analytical method, numerical method, rectangular enclosure, shielding effectiveness, and transmission line theory.

I. INTRODUCTION

Shielding is a useful and simple technique in EMC field. As to common electronic equipment, its metallic enclosure usually has one or more apertures, which break the completeness of metallic enclosure. How to evaluate the shielding effectiveness (SE) of the enclosure and analyze the factors that affect the SE, becomes a practical problem.

At present, there are three kinds of methods that can be utilized to investigate the SE, including methods based on Bethe's small hole theory, numerical methods, and analytical methods. As early as 1970's, Mendez [1, 2] proposed an analytic shielding formulation for rectangular enclosures excited by internal sources. Using the well-known Bethe's small hole theory [3], Mendez replaced the apertures by equivalent electric and magnetic dipoles. However, this approach is limited to small holes/apertures and is only valid for frequencies below the first resonance. To overcome the limitation of the small hole theory approximation, Wallen *et al*. [4] employed cavity Green's functions to extend Mendez's approach to include the cavity resonance region. Audone and Balma [5] also considered a similar analysis to [4] for a rectangular enclosure with an aperture using MOM along with a network formulation. However, these analyses were still limited to frequencies below the first resonance.

More recently, numerical methods such as transmission line method (TLM), finite-element method(FEM), moment method (MOM), finite-difference time-domain method (FDTD), and the hybrid methods are used in the calculation of SE [6-11]. Numerical methods can offer good accuracy over a broad frequency band but at the cost of large memory and computational time. Hence, numerical methods are severely limited when it comes to analyzing practical enclosures with large number of small holes.

Submitted On: Aug. 19, 2012
Accepted On: Apr. 13, 2013

Another analytical method proposed by Robinson *et al.* [12], is based on transmission line theory and used in the calculating of SE. Although the accuracy, this method can be only applied to simple geometries with use of approximations, while it can be used to analyze the effects of many factors on SE. The computation time and computer memory are also saved, which are very useful for the engineers that design the metallic enclosure.

In this paper, for an enclosure with apertures, an accurate aperture array admittance for use in the waveguide equivalent circuit model of Robinson *et al.* is presented. The enclosure is modeled as a short-circuited waveguide, the aperture array is characterized by an admittance. Additionally, the incident wave is modeled by a voltage source and free-space impedance in the equivalent circuit. Using this circuit model, SE for an off-center aperture, aperture array, high-order modes, enclosure loss, arbitrary incident angles, and polarization angles can be calculated. Then, main factors that affect the SE are analyzed, which can be referenced for the design and EMC of electronic equipment's enclosure.

II. TRANSMISSION LINE METHOD OF CALCULATING SE OF RECTANGULAR ENCLOSURE WITH APERTURE(S)

A. Enclosure with only one aperture

Based on Robinson *et al*'s method [12], the enclosure with one aperture (Fig. 1 (a)) can be modeled in Fig. 1 (b). The electric shielding at a distance p from the aperture is obtained from the voltage at a point P in the equivalent circuit, while the current at P gives the magnetic shielding. The radiating source is represented by voltage V_0 and impedance $Z_0 = 377\ \Omega$, and the enclosure by the shorted waveguide whose characteristic impedance and propagation constant are Z_{mg} and k_{mg}, respectively. The load impedance Z_l is included in this circuit model, which represents the loss of enclosure.

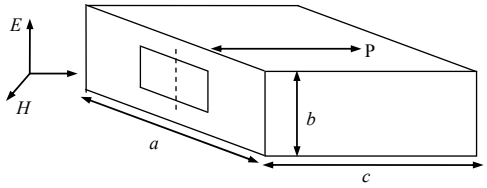

(a) Rectangular enclosure with one aperture.

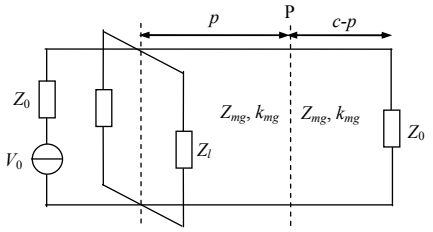

(b) Equivalent circuit.

Fig. 1. Rectangular enclosure with one aperture and its equivalent circuit.

The aperture is represented as a length of coplanar strip transmission line. According to Gupta's theory [13], the characteristic impedance of the transmission line can be given by,

$$Z_{os} = 120\pi^2 \left[\ln\left(2\frac{1+\sqrt[4]{1-(w_e/b)^2}}{1-\sqrt[4]{1-(w_e/b)^2}} \right) \right]^{-1}. \quad (1)$$

The effective width is given by

$$w_e = w - \frac{5t}{4\pi}\left(1 + \ln\left(\frac{4\pi w}{t}\right)\right), \quad (2)$$

where t is the thickness of enclosure wall, w is the width of the aperture.

To calculate the aperture impedance Z_{ap}, we transform the load impedance Z_l at the end of the aperture in considering a distance $l/2$ to the centre,

$$Z_{ap} = \frac{1}{2} C_m Z_{os} \frac{Z_l + jZ_{os}\tan(k_0 l/2)}{Z_{os} + jZ_l \tan(k_0 l/2)}. \quad (3)$$

Figure 2 shows the coordinate system of the aperture, where l and w are the length and width of the aperture, respectively. X and Y are the aperture positions from the origin to the centre of the aperture, respectively. According to field continuity at the aperture, the coupling coefficient C_m [14] is introduced to account for higher-order modes and the coupling between the aperture and the enclosure, so the SE for off-centre aperture and higher order modes can be calculated.

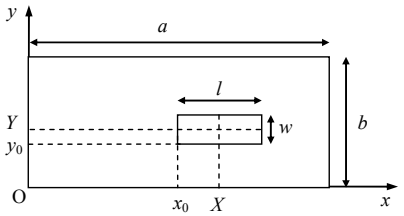

Fig. 2. Coordinate system of the aperture.

In many studies, the enclosure is modeled as a perfect conductor, whose conductivity is infinite, then Z_l = 0. But for a practical material, its impedance should be described as

$$Z_l = (1+j)\sqrt{\pi f \mu_1 / \sigma_1}\,, \tag{4}$$

where μ_1 and σ_1 are magnetic permeability and conductivity of the enclosure, respectively.

Based on Thevenin's theorem, combining Z_0, V_0 and Z_{ap} gives an equivalent voltage and its impedance

$$V_1 = V_0 Z_{ap} /(Z_0 + Z_{ap}), \tag{5}$$

$$Z_1 = Z_0 Z_{ap} /(Z_0 + Z_{ap})\,. \tag{6}$$

Now transform V_1, Z_1 at the end of the waveguide to P, giving equivalent voltage V_2 and source impedance Z_2

$$V_2 = \frac{V_1}{\cos(k_{mg} p) + j(Z_1 / Z_{mg})\sin(k_{mg} p)}, \tag{7}$$

$$Z_2 = Z_{mg} \frac{Z_1 + jZ_{mg}\tan(k_{mg} p)}{Z_{mg} + jZ_1 \tan(k_{mg} p)}. \tag{8}$$

For the TE_{mn} mode of propagation, the waveguide's characteristic impedance and propagation constant respectively are

$$\begin{cases} Z_{mg} = Z_0 / \sqrt{1-(m\lambda/2a)^2 - (n\lambda/2b)^2}, \\ k_{mg} = k_0 \sqrt{1-(m\lambda/2a)^2 - (n\lambda/2b)^2}, \end{cases} \tag{9}$$

where $k_0=2\pi/c$, and c is velocity of light in free space.

Now transform the equivalent impedance of the enclosure wall to P, giving load impedance Z_3,

$$Z_3 = Z_{mg} \frac{Z_l + jZ_{mg}[k_{mg}(c-p)]}{Z_{mg} + jZ_l[k_{mg}(c-p)]}. \tag{10}$$

Then we can get the voltage at P by

$$V_{pm} = \frac{V_2 Z_3}{Z_2 + Z_3}. \tag{11}$$

The current at P is

$$I_{pm} = \frac{V_2}{Z_2 + Z_3}. \tag{12}$$

For all the wave modes in the enclosure, the total voltage at P is

$$V_{ptotal} = \sum V_{pm}. \tag{13}$$

And the total current at P is

$$I_{ptotal} = \sum I_{pm}. \tag{14}$$

In the absence of the enclosure, the load impedance at P is Z_0, the voltage and current at P are $V_p=V_0/2$ and $I_p=V_0/2Z_0$, respectively. Then the electric shielding and the magnetic shielding are given by

$$SE = 20\lg\left|V_{ptotal}/V_p\right| = 20\lg\left|V_0/2V_p\right|, \tag{15}$$

$$SM = 20\lg\left|I_{ptotal}/I_p\right| = 20\lg\left|V_0/2Z_0V_p\right|. \tag{16}$$

B. Enclosure with an array of apertures

(1) *With an array of rectangular apertures*

Sometimes, the enclosure has an array of identical rectangular apertures, as shown in Fig. 3.

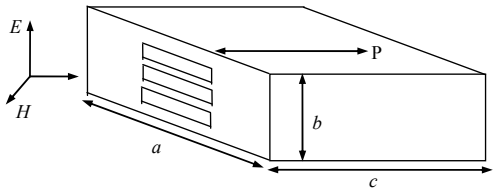

Fig. 3. Enclosure with an array of rectangular apertures.

If the apertures are distant from each other, the aperture array's impedance Z'_{ap} is calculated by

$$Z'_{ap} = kZ_{ap}, \tag{17}$$

where k is the number of apertures. Equation (17) shows that the aperture array's impedance is the sum of that of each aperture. By replacing Z_{ap} in section A with Z'_{ap}, the SE is derived.

(2) *With an array of round apertures*

Sometimes, the enclosure may have an array of round apertures, as shown in Fig. 4.

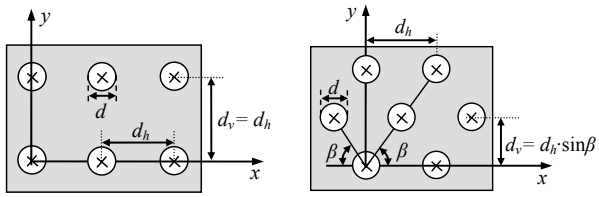

Fig. 4. Geometry of the enclosure with an array of round apertures arranged in the center of enclosure wall (square arrangement or at an angle of β).

In Fig. 4, the array of apertures can be represented by an appropriate admittance. Taking the mutual coupling between apertures into account and the normalized shunt admittance for both configurations is [15, 16],

$$\frac{Y_{ap}}{Y_0} = -j\frac{3d_h d_v \lambda_0}{\pi d^3} + j\frac{288}{\pi\lambda_0 d^2} \cdot \left[\sum_{\substack{m=0 \\ m\neq odd}}^{\infty}\sum_{\substack{n=0 \\ n\neq odd}}^{\infty}\left(\frac{\varepsilon_m n^2}{d_v^2} + \frac{\varepsilon_n m^2}{d_h^2}\right)J_1^2(X)\right], \quad (18)$$

where λ_0 and Y_0 are the free-space wavelength and intrinsic admittance, respectively, d_v and d_h are the vertical and horizontal aperture separations assuming that aperture's diameter d is smaller than the separations.

In equation (18), $X = \frac{[\pi d(m^2/d_h^2 + n^2/d_v^2)/2]^{1/2}}{(m^2/d_h^2 + n^2/d_v^2)^{5/2}}$, and the primes denote summation on even integers only, J_1 is the Bessel function of the first kind of the first order, and $\varepsilon_{m,n}$= 1 if m, n = 0 and 2 if m, $n\neq 0$. The second term in equation (18) can be neglected when d_v, d_h and d are much smaller than the wavelength.

In Fig. 4, the effective wall impedance Z'_{ap} is a fraction of Z_{ap}. Using an impedance ratio concept, Z'_{ap} becomes

$$Z'_{ap} = Z_{ap} \times \frac{l \times w}{a \times b}, \quad (19)$$

where l and w are the length and width of the array, respectively, and they are given by

$$l = d/2 + (k_1 - 1)d_h + d/2, \quad (20)$$

$$w = d/2 + (k_2 - 1)d_v + d/2, \quad (21)$$

where k_1 and k_2 are the number of apertures in length and width direction of the array, respectively. If the apertures are staggered arranged by an angle β, then $d_v = d_h \cdot \sin\beta$.

C. SE for any polarization angles and incident angles plane wave

It is worth noting that polarization angles are not considered in Robinson *et al.*'s method in the earlier analysis, and the plane wave is supposed as perpendicularly illuminating the enclosure wall with aperture(s).

If the plane wave is polarized at an angle φ, then the incident plane wave E can be divided into two components, which are vertical polarization component $E_v = E\cdot\sin\varphi$ and horizontal polarization component $E_h = E\cdot\cos\varphi$. Based on electromagnetic theory, the electric field propagation coefficient is

$$T = \frac{2Z_2}{Z_2 + Z_1}. \quad (22)$$

Equation (22) shows that when the wave illuminates a dividing boundary of two mediums, one part is reflected, and one part penetrates into the other medium. As to E_v, the penetration part is calculated as follows. The equivalent impedance can be calculated as that in section A for single aperture and section B for aperture array.

When the plane wave obliquely illuminates the enclosure wall with aperture(s) at an angle θ, Z_2 in equation (22) is given by $Z_2 = Z_{ap}/\cos\theta_T$, and $\cos\theta_T = \sqrt{1 - (\varepsilon_1 \sin^2\theta)/\varepsilon_2}$. Here, ε_1 and ε_2 are the electric permeability of the two medias. When the plane wave propagates from air into the enclosure, ε_1 is the electric permeability of air, and ε_2 is the equivalent electric permeability of aperture(s), $\varepsilon_2 = \mu_0 / Z_{os}^2$. μ_0 is the equivalent magnetic permeability of the aperture(s), and it's equivalent to that of air. Z_1 in equation (22) is given by $Z_1 = Z_0/\cos\theta$. Then, the vertical electric field propagation coefficient T_v is given by,

$$T_v = \frac{2Z_2}{Z_2 + Z_1} = \frac{2Z_{ap}/\cos\theta_T}{Z_0/\cos\theta + Z_{ap}/\cos\theta_T}. \quad (23)$$

The vertical polarization component of electric field after penetrating the aperture(s) is given by $E_v^1 = T_v E_v$. As to E_h, Z_1 and Z_2 in equation (22) are respectively given by $Z_1 = Z_0\cos\theta$ and $Z_2 = Z_{ap}\cos\theta_T$. Then, the horizontal electric field propagation coefficient T_h is given by,

$$T_h = \frac{2Z_2}{Z_2 + Z_1} = \frac{2Z_{ap}\cos\theta_T}{Z_0\cos\theta + Z_{ap}\cos\theta_T}. \quad (24)$$

The horizontal polarization component of electric field penetrating the aperture(s) is given by $E_h^1 = T_h E_h$. The equivalent circuits of the vertical polarization and horizontal polarization components of electric field propagating in the enclosure are given by Figs. 5 (a) and 5 (b), respectively.

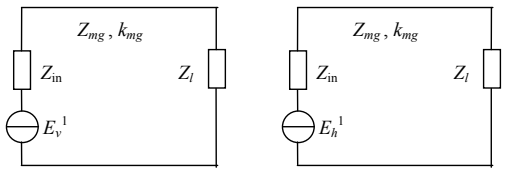

(a) (b)

Fig. 5. Equivalent circuits of vertical polarization and horizontal polarization components of electric field propagating in the enclosure.

The electric voltage at P can be calculated as that in section A. For vertical polarization and horizontal polarization components of electric field, the total voltage are respectively given by $V_v^{total} = \sum V_v^{pm}$ and $V_h^{total} = \sum V_h^{pm}$. Then the total voltage at P is given by $V_{total} = \sqrt{(V_v^{total})^2 + (V_h^{total})^2}$, and the SE can be calculated using equations (15) and (16).

III. EXAMPLE AND ANALYSIS

Unless other specified, the simulation parameters are characterized as: the dimensions of enclosure is 300 × 120 × 300 mm^3, thickness of enclosure wall made of copper is t = 1.5 mm. The coordinate of observation point P is x = 225 mm, y = 60 mm and z = 140 mm. The plane wave perpendicularly illuminates the enclosure wall with aperture(s).

A. Single aperture case

For the validation of the proposed method, we consider a rectangular aperture, whose dimensions are 50 × 5 mm^2 (unless other specified, the aperture dimensions in the following is stationary). From Fig. 6, it can be observed that the calculated result using the proposed method is in well agreement with the results from [17].

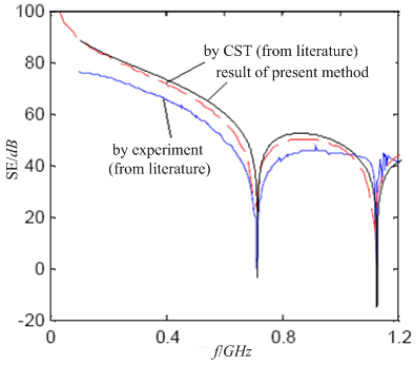

Fig. 6. Validation of present method for single aperture case.

(1) *Effect of aperture dimensions on SE*

Figure 7 shows that the SE becomes worse when the dimension of the aperture is enlarged. When the frequency is about 707 MHz and 1.12 GHz, the SE is negative, which is caused by resonance. The resonance frequency is calculated by,

$$f = \frac{1}{2\sqrt{\mu\varepsilon}}\sqrt{\left(\frac{m}{a}\right)^2 + \left(\frac{n}{b}\right)^2 + \left(\frac{l}{c}\right)^2}, \qquad (25)$$

where m, n, and l are determined by the wave modes in the enclosure. Using equation (25), we can get the resonance frequency point is 707 MHz for TE_{101} mode, and 1.12 GHz for TE_{201} mode. Based on microwave theory, it is known that the SE at resonance frequency will become negative which leads to the least value of SE.

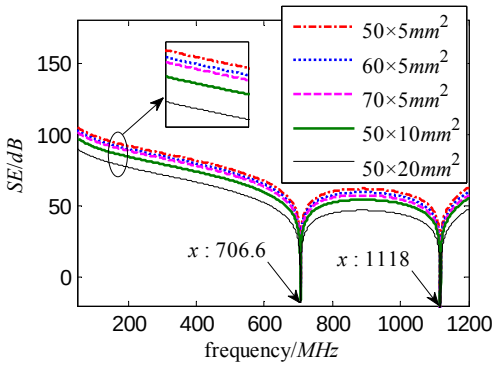

Fig. 7. Effect of aperture dimensions on SE.

(2) *Effect of enclosure dimension on SE*

The thickness of enclosure wall is 1 mm, Fig. 8 shows SE for different enclosure dimensions.

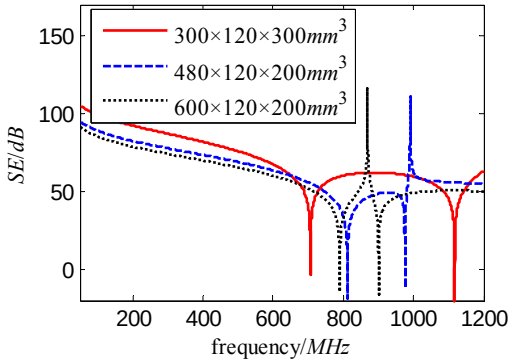

Fig. 8. Effect of enclosure dimensions on SE.

Using equation (25), we can deduce that in the frequency band of 0~1.2 GHz, the three enclosures all have two resonance frequencies. The resonance frequencies of first enclosure are about 707 MHz and 1.12 GHz, those of the second are about 312.3 MHz and 624.6 MHz, and those of the third are about 249.9 MHz and 499.7 MHz. All the upper resonance frequencies can be found from Fig. 8. The SE is negative at resonance frequencies, and

does not change monotonously as the enclosure is enlarged.

(3) *Effect of observation point's position on SE*

When the frequencies of the plane wave is f = 0.75 GHz, 0.90 GHz or 1.20 GHz, as p changes, the SE at point P is shown in Fig. 9.

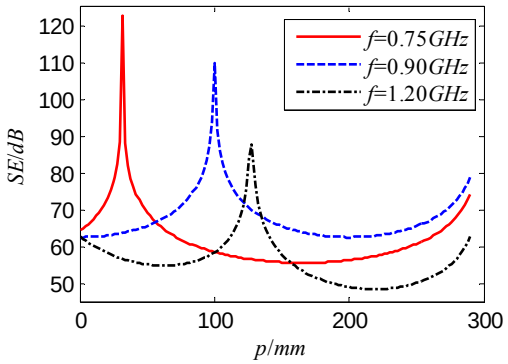

Fig. 9. Effect of observation point's position on SE.

It is shown that the SE does not change as intuition or literatures [18, 19]: the SE is better when p is larger. The SE does not monotonously reduce or increase as p changes. When the frequency of the incident plane wave is f = 0.75 GHz, there is only TE_{10} mode in the enclosure, the SE is best when p = 32 *mm*, and worst when p = 164 *mm*. When f = 0.90 GHz, there is also only TE_{10} mode in the enclosure, the SE is best when p = 100 *mm*, and worst when p = 201 *mm*. When f = 1.20 GHz, there are TE_{10} and TE_{20} modes in the enclosure, the SE is best when p = 128 *mm*, and worst when p = 216 *mm*. So we know that the SE is not only related with p, but also with frequency of incident plane wave. Based on electromagnetic theory, we can get the following laws.

For the TE_{mn} or TM_{mn} mode in the enclosure, the SE is worst when

$$p_{\min} = c - i\lambda_y / 4, \quad i = 1,3,5,\cdots,$$

and the SE is best when

$$p_{\max} = c - i\lambda_y / 2, \quad i = 0,1,2,\cdots,$$

where $\lambda_y = 2/\sqrt{(2f/c)^2 - (m/a)^2 - (n/b)^2}$.

It can be observed that the sensitive component can be set based on the upper laws.

(4) *Effect of aperture's position on SE*

Figure 10 shows the SE for the same aperture at three different positions. In conclusion, the SE of the middle aperture is the worst. The nearer the aperture is to the edge the better SE is obtained. This model allows us to determine the SE not only in the centre of the enclosure but also for any other positions, which is impossible with Robinson *et al*'s model. Based on the results, electronic engineers should place apertures at the edges of the enclosure.

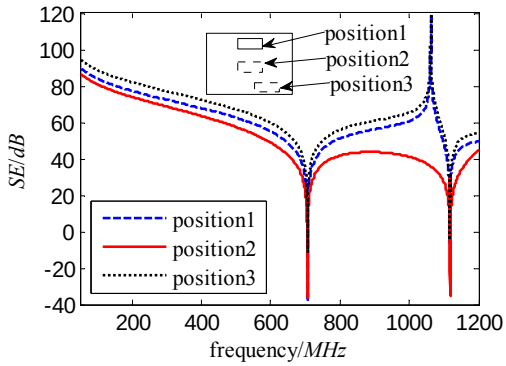

Fig. 10. Effect of aperture's position on SE.

(5) *Effect of enclosure wall's thickness and material conductivity on SE*

When the enclosure wall's thickness t and material conductivity are changed, respectively, the SE are shown in Figs. 11 (a) and 11 (b). Figure 11 (a) shows that the SE is better as t is increased. This is because when t is increased, electromagnetic energy penetrating into the enclosure is decreased. But t only has a little effect on SE. Figure 11 (b) shows when increasing the material conductivity, the SE is stationary.

(6) *Effect of ratio between aperture's length and width*

The thickness of enclosure wall is 1 *mm*. The area of aperture is 250 mm^2, and the dimensions of aperture is 50 × 5 mm^2, 15.8 × 15.8 mm^2 or 5 × 50 mm^2, respectively. Figure 12 shows that SE is better when the ratio of aperture's length and width is reduced. This is because electromagnetic energy transmitted into the enclosure is decreased when decreasing the ratio.

B. An array of apertures case

For the validation of the proposed method in the case of apertures array, we consider an enclosure with one large aperture or three smaller ones located at center of its side wall. The three

smaller apertures are identical, with dimensions of $10 \times 1.0\ cm^2$ and their vertical separation d is 2 cm. The area of the large aperture is equal to the total areas of the three apertures. Figure 13 shows that the results calculated by present method are in well agreement with the results from [20].

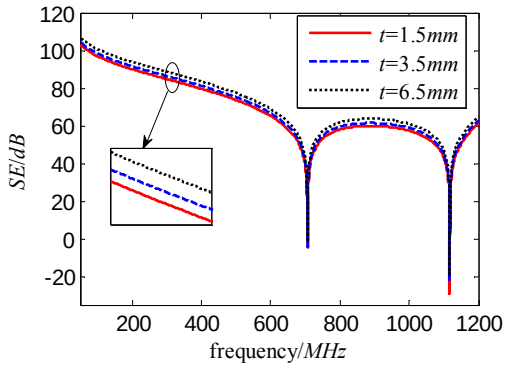

(a) Effect of enclosure wall's thickness.

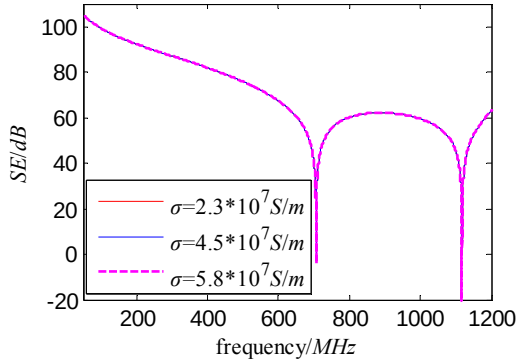

(b) Effect of material conductivity.

Fig. 11. Effect of enclosure wall's thickness and material conductivity on SE.

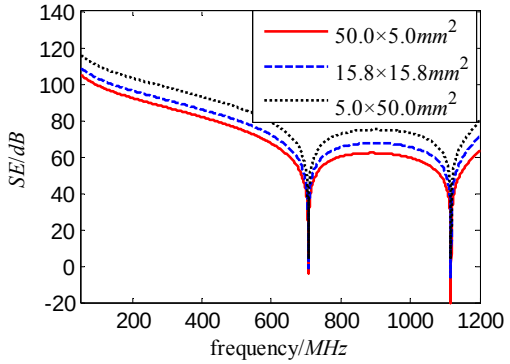

Fig. 12. Effect of ratio of aperture's length and width.

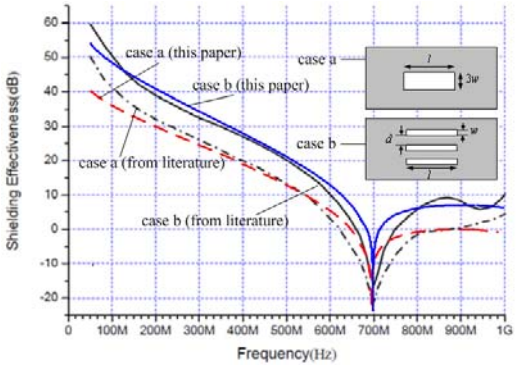

Fig. 13. Validation of present method for aperture array case.

(1) *Effect of aperture shape on SE*

Case 1: the number of rectangular apertures is $k = 3$, and the dimensions of each aperture is $50 \times 10\ mm^2$. Case 2: the number of square arrangement round apertures shown in Fig. 4 is 5×3, the distance between two adjacent apertures is $d_v = d_h = 20\ mm$, the radius of each aperture is about 5.64 mm in order to guarantee that the total area of round apertures is equivalent to that of rectangular apertures in case 1. Figure 14 shows that if the area of rectangular and round apertures are equivalent, the SE is better for round apertures.

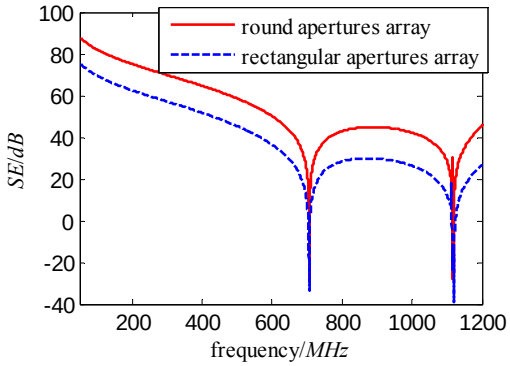

Fig. 14. Effect of aperture shape on SE.

(2) *Effect of number of round apertures on SE*

An enclosure wall has an array of round apertures, when d_v, d_h, and the total area of apertures S_1 are stationary, only the diameter of aperture d is variable, Fig. 15 (a) shows the SE for three cases. When the area of apertures array S_2 and the diameter of aperture d are stationary, only the number of apertures is variable, Fig. 15 (b) shows the SE for this case.

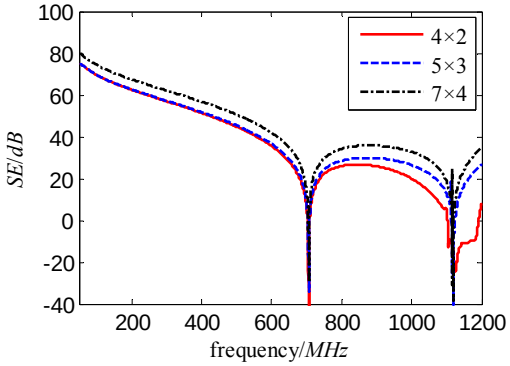

(a) d_v, d_h and S_1 are stationary, only the number of apertures is variable.

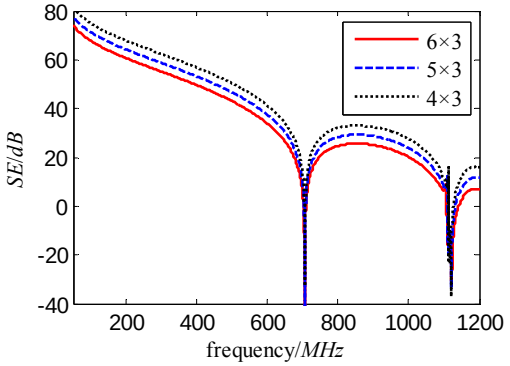

(b) S_2 and d are stationary, only the number of apertures is variable.

Fig. 15. Effect of number of round apertures on SE.

Figure 15 (a) shows that when d_v, d_h and S_1 are stationary, by reducing the diameter of round aperture, the SE can be improved. Figure 15 (b) shows that when S_2 and d are stationary, by reducing the distance d_v and d_h, and increasing the number of apertures, the SE is reduced.

(3) *Effect of rectangular apertures' number on SE*

The enclosure has an array of rectangular apertures, and there are three cases of the array. Case 1: dimensions of aperture is $l \times w = 50 \times 5$ mm^2, the apertures' number k is variable. Case 2: total area of apertures and aperture length l are stationary, aperture width w and number of apertures k are variable. Case 3: total area of apertures and aperture width w are stationary, the aperture length l and number of apertures k are variable. Figures 16 (a), (b), and (c) shows the SE for the three cases, respectively.

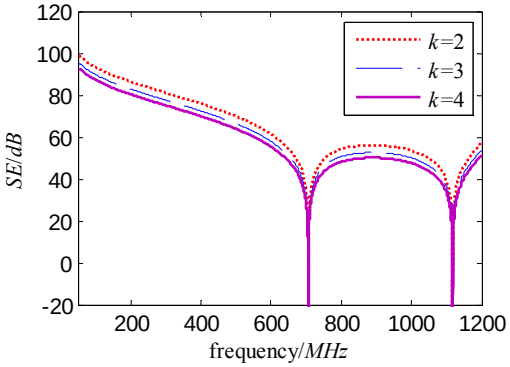

(a) The area of single aperture is stationary, and number of apertures is variable.

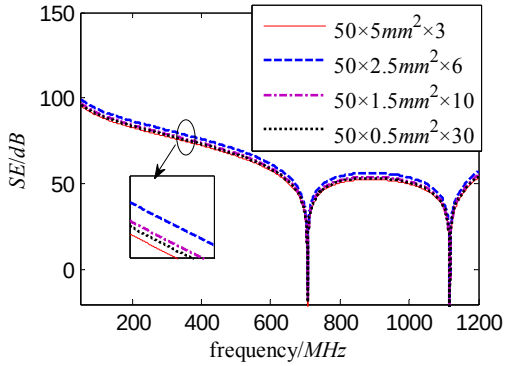

(b) Total area of apertures is stationary, the width of aperture and number of apertures are variable.

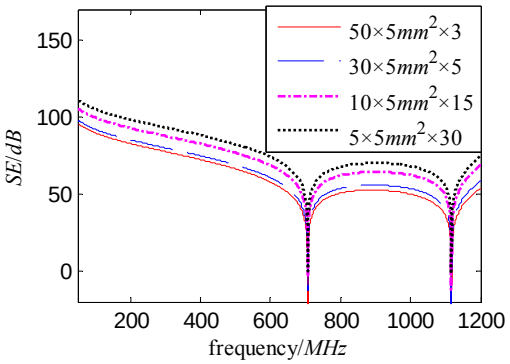

(c) Total area of apertures is stationary, the length of aperture and number of apertures are variable.

Fig. 16. Effect of rectangular apertures' number.

Figure 16 (a) shows that if the area of single aperture and ratio of aperture length and width are stationary, the SE is reduced with increasing the number of apertures. Figure 16 (b) shows that if the area of apertures and aperture length are stationary, by reducing the aperture width, the

number of apertures is increased, but the SE is not changed monotonously for this case. Figure 16 (c) shows that if the area of apertures and aperture width are stationary, by reducing the aperture length, the number of apertures is increased, then the SE is improved.

(4) *Effect of aperture array's arrangement on SE*

There is an aperture array that contains square and round apertures, and it is arranged by two styles. The radius of round aperture is r = 5 *mm*, and the length of square aperture is w = 1 *cm*. The adjacent apertures are distant from each other. Figure 17 shows the SE is stationary when the arrangement of apertures is changed.

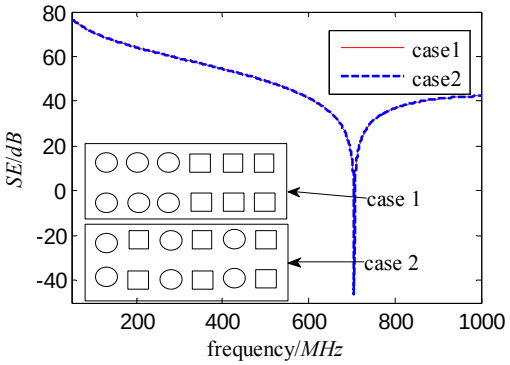

Fig. 17. Effect of aperture array's arrangement on SE.

C. Effect of polarization angles and incident angles on SE

Suppose that there is an aperture at the center of the enclosure wall. The dimensions of the aperture are 100 × 5 mm^2. The frequency and incident angle θ of incident plane wave is 700 MHz and 90^0, respectively, when polarization angle φ varies from 0^0 to 88^0, the SE is depicted in Fig. 18 (a). It can be observed that the results calculated by present method and that from [21] are consistent, which validates the proposed method.

Figure 18 (b) shows the SE for the case that polarization angle φ of incident plane wave is 30^0, 45^0, and 60^0, respectively, and incident angle θ changes from 0^0 to 180^0. It's shown that when θ changes from 0^0 to 90^0, the SE is improved. When θ changes from 90^0 to 180^0, the SE is reduced.

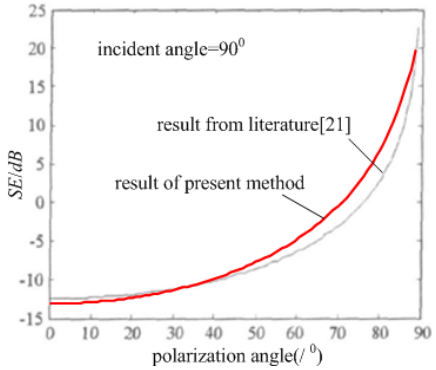

(a) Effect of polarization angles.

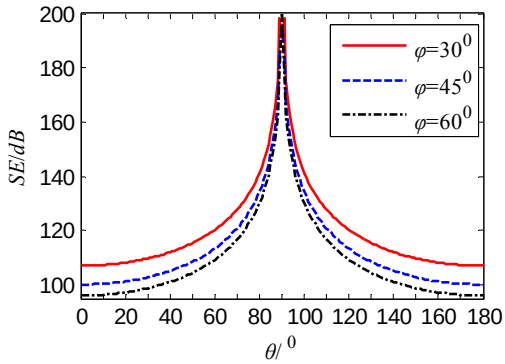

(b) Effect of incident angles.

Fig. 18. Effect of polarization angles and incident angles on SE.

IV. CONCLUSION

In this paper, an efficient analytical approach based on Robinson *et al.*'s model has been presented to predict the SE of enclosures with off-centre apertures, numerous apertures, and for any polarization angles and incident angles plane wave. The calculation of the electric shielding depends on the frequency, polarization, and incident angles of the incident wave, the dimensions of the enclosure and the aperture(s), the number of apertures, the degrees of closeness, the position of aperture(s), etc. The method described in this paper has good agreement with other methods over a wide frequency range. The estimation of the SE based on the proposed method has offered a cost-effective alternative to the numerical techniques through saving computing resources. Solution time is the key advantage of the proposed model. Therefore, this study may be helpful in designing an effective shield to achieve better shielding performance.

ACKNOWLEDGMENT

This research was supported by Natural Science Foundation of China (Grant Number: 50977091).

REFERENCES

[1] H. A. Mendez, "On the theory of low-frequency excitation of cavity resonances," *IEEE Trans. Microwave Theory Tech*., vol. 18, pp. 444-448, 1970.

[2] H. A. Mendez, "Shielding theory of enclosures with apertures," *IEEE Trans. Electromagn. Compat.*, vol. 20, pp. 296-305, May 1978.

[3] H. A. Bethe, "Theory of diffraction by small holes," *Phys. Rev.* II, vol. 66, pp. 163-182, 1944.

[4] W. Wallyn, D. De Zutter, and E. Laermans, "Fast shielding effectiveness prediction for realistic rectangular enclosures," *IEEE Trans. Electromagn. Compat.*, vol. 45, no. 4, pp. 639-643, 2003.

[5] B. Audone and M. Balma, "Shielding effectiveness of apertures in rectangular cavities," *IEEE Trans. Electromagn. Compat.*, vol. 31, no. 1, pp. 102-106, 1989.

[6] Jr. W. P. Carpes, G. S. Ferreira, and A. Raizer, *et al*, "TLM and FEM methods applied in the analysis of electromagnetic coupling," *IEEE Trans. Magn.*, vol. 36, no. 4, pp. 982-985, 2000.

[7] V. Rajamani, C. F. Bunting, and M. D. Deshpande, *et al*, "Validation of modal/ MoM in shielding effectiveness studies of rectangular enclosures with apertures," *IEEE Trans. Electromagn. Compat.*, vol. 46, no. 2, pp. 348-353, 2006.

[8] J. Chen and A. X. Zhang, "A Subgridding scheme based on the FDTD method and HIE-FDTD method," *Appl. Comp. Electro. Society (ACES) Journal*, vol. 26, no. 1, pp. 1-7, 2011.

[9] W. Abdelli, X. Mininger, and L. Pichon, *et al*, "Impact of composite materials on the shielding effectiveness of Enclosures," *Appl. Comp. Electro. Society (ACES) Journal*, vol. 27, no. 4, pp. 369-375, 2012.

[10] P. Dehkhoda, A. Tavakoli, and M. Azadifar, "Shielding effectiveness of an enclosure with finite wall thickness and perforated opposing walls at oblique incidence and arbitrary polarization by GMMoM," *IEEE Trans. Electromagn. Compat.*, vol. 54, no. 4, pp. 792-805, 2012.

[11] N. Fichtner and P. Russer, "A hybrid TLM-integral equation method using time–domain plane-waves for shielding effectiveness computations," *26th Annual Review of Progress in Appl. Comp. Electro. Society (ACES)*, Tampere, Finland, pp. 404-409, April, 2010.

[12] M. P. Robinson, T. M. Benson, and C. Christopoulos, *et al*, "Analytical formulation for the shielding effectiveness of enclosures with apertures," *IEEE Trans. Electromagn. Compat.*, vol. 40, no. 3, pp. 240-248, 1998.

[13] K. C. Gupta, R. Garg, and I. J. Bahl, *Microstrip Lines and Slot Lines*, Artech House, Norwood, MA, 1979, Ch.7.

[14] D. Shi, Y. Shen, and Y. Gao, "3 High-order mode transmission line model of enclosure with off-center aperture," *IEEE Int. Symp. on Electromagn. Compat.*, pp. 361-364, October, 2007.

[15] T. Y. Otoshi, "A study of microwave leakage through perforated flat plates," *IEEE Trans. Microw. Theory Tech.*, vol. 20, no. 3, pp. 235-236, 1972.

[16] W. Culshaw, "Reflectors for a microwave Fabry–Perot interferometer," *IEEE Trans. Microw. Theory Tech.*, vol. 7, no. 2, pp. 221-228, 1959.

[17] X. H. Chen, "Research on composite shielding effectiveness computing method and equipments electromagnetic protection envelope," *Doctoral Thesis of Shi Jia Zhuang, Mechanical Engineering College*, China, 2011.

[18] H. Song, D. F. Zhou, and D. T. Hou, *et al*, "Hybrid algorithm for slot coupling of double layer shielding cavity," *High Power Laser and Particle Beams*, vol. 20, no. 11, pp. 1892-1898, 2008.

[19] L. Wang and Y.Gao, "Analysis of shielding effectiveness for rectangular cavity with apertures and resonance suppression," *Chinese Journal of Radio Science*, vol. 23, no. 3, pp. 560-564, 2008.

[20] G. Wu, X. Zhang, and B. Liu, "A Hybrid method for predicting the shielding effectiveness of rectangular metallic enclosures with thickness apertures," *J. of Electromagn. Waves and Appl.*, vol. 24, pp. 1157-1169, 2010.

[21] X. F. Zhang, Y. Li, and G. Y. Ni, *et al*, "Hybrid model to evaluating shielding effectiveness of cavity with apertures," *Chinese Journal of Radio Science*, vol. 26, no. 1, pp. 25-29, 2011.

Chuan-Chuan Wang received the B. A. and M. Sc. degrees in Electrical Engineering from Shi Jia Zhuang, Mechanical Engineering College, China, in 2007 and 2009, respectively. He is currently working toward the Ph.D. degree in electromagnetic protection engineering in Shi Jia Zhuang, Mechanical Engineering College. His research interests include transmission-line theory, EMC, and EM protection.

Chang-Qing Zhu received the M.Sc. degree in Measurement Engineering from the North University of China, Shan xi, China, in 1987, and the Ph.D. degree in electromagnetic protection engineering from Shi Jia Zhuang, Mechanical Engineering College, China, in 2005.

He is currently a Professor in the Mechanical Engineering College. His current research interests include Test of Electromagnetic field, Automation of electrical system, and EMC.

Xing Zhou received the M.Sc. degree in Electrical Engineering from National University of Defense Technology, Hunan, China, in 2002, and the Ph.D. degree in electromagnetic protection engineering from Shi Jia Zhuang, Mechanical Engineering College, China, in 2006.

She is currently a Lecturer in Shi Jia Zhuang, Mechanical Engineering College. Her research interests include transmission-line theory, EMC, and EM protection.

Zhi-Feng Gu received the B. A. and M. Sc. degrees in Electrical Engineering from Hebei University of Technology, Tian jin, China, in 2002 and 2005, respectively.

He is currently a Lecturer and working toward the Ph.D. degree in control engineering at the Shi Jia Zhuang, Mechanical Engineering College. His research interests include control theory and techniques, and automation of electrical system.